The main role of the ZrO_2–MgO–CaO and ZrO_2–MgO–CaO–SiO_2 systems in the field of refractories

Carmen Baudín*, Pilar Pena

Instituto de Cerámica y Vidrio, CSIC, 28049 Madrid, Spain

ABSTRACT

The increasing severity of the working conditions of refractories together with the necessity of available and economically feasible raw materials have changed the design approaches towards materials experiencing "in situ" modifications during use.

The systems ZrO_2–MgO–CaO and ZrO_2–MgO–CaO–SiO_2 are key ones in refractory technology due to the high temperatures for liquid formation involved. Apart from the well-known ZrO_2, MgO, MgO-C and MgO·CaO commercial refractories, calcium zirconate (CZ, $CaZrO_3$)-based materials have been proposed due to the low thermal conductivity and high refractoriness of CZ. Naturally occurring minerals as dolomite, baddeleyite or zircon are potential raw material candidates for the fabrication of relatively low cost MgO-CZ-based refractories.

This work discusses guidelines for the formulation of basic refractories with CZ-based matrices. The effect of composition on the microstructural development, the mechanical behaviour and the corrosion resistance against cement clinker are discussed.

© 2021 SECV. Published by Elsevier España, S.L.U. This is an open access article under the CC BY-NC-ND license (http://creativecommons.org/licenses/by-nc-nd/4.0/).

El papel clave de los sistemas ZrO_2-MgO-CaO y ZrO_2-MgO-CaO-SiO_2 en el sector de los refractarios

RESUMEN

El incremento en la severidad de las condiciones de trabajo de los nuevos materiales refractarios y la necesidad de disponer de materias primas económicamente viables, han dado lugar a cambios en el enfoque del diseño microestructural hacia materiales que experimentan modificaciones «in situ» durante su uso.

* Corresponding author.
  E-mail address: cbaudin@icv.csic.es (C. Baudín).

Los sistemas ZrO$_2$-MgO-CaO y ZrO$_2$-MgO-CaO-SiO$_2$ son clave en la tecnología refractaria debido a las altas temperaturas de formación de líquidos involucradas. Además de los refractarios comerciales ZrO$_2$, MgO, MgO-C y MgO.CaO, se han propuesto materiales a base de circonato cálcico (CZ, CaZrO$_3$) debido a la baja conductividad térmica y alta refractariedad del CZ. Los minerales como la dolomita, la baddeleyita o el circón son candidatos potenciales a materias primas para la fabricación de refractarios basados en MgO-CZ de costo relativamente bajo.

Este trabajo analiza las pautas para la formulación de refractarios básicos con matrices basadas en CZ. Se discute el efecto de la composición sobre el desarrollo microestructural, el comportamiento mecánico y la resistencia a la corrosión frente al clínker de cemento.

Introduction

The European ceramics sector accounts for EUR 27.8×10^3 million in production value and it provides over 338 thousand jobs (https://ec.europa.eu/growth/sectors/raw-materials/industries/non-metals/ceramics_es). Refractories constitute one of the major value sectors (17%), just after building ceramics – wall and floor tiles (31%) and bricks and roof tiles (20%) – (http://cerameunie.eu/ceramic-industry/facts-figures/).

Refractories are essential for all high-temperature industrial processes. Their role is three-fold as they provide structural integrity, corrosion resistance and thermal insulation. Main industries such as production of steel, aluminium, glass, ceramics, cement, chemicals and energy, and waste management, involve some of the most aggressive high-temperature environments, thus, refractories are strategic materials for them.

Consequently, the evolution of refractories has always been linked to requirements of other industries in order to reach higher quality or productivity and, in the last years, related to occupational health and environmental issues such as waste and emissions. In general, in modern refractory practice relatively expensive materials that last long time are preferred to short-life cheap ones.

Since refractories are fabricated in large quantities and sizes the use of high purity raw materials is not commercially viable. Moreover, it is not technologically necessary because properly designed refractory compositions and microstructures support the envisaged solicitations, as will be described in this work. Synthetic raw materials are used for the fabrication of some refractories (e.g.: ZrO$_2$, MgO, Al$_2$O$_3$, SiC), however, most refractories are fabricated from beneficied (purified, milled, compacted and heat treated) ores (e.g.: mullite-based chamottes, bauxite, doloma) or natural ores with carefully controlled composition and grain size (e.g.: zircon, andalusite, clays).

During use, refractories are subjected to extreme environments that give rise to a combination of thermochemical and thermomechanical solicitations. The word "refractory", which comes from stubborn (refractarius in Latin), describes well the original approach for their designing as materials resistant to the extreme conditions by being chemically and physically stable under the environmental conditions.

The solicitations at which refractories are subjected have progressively become more severe to reach the higher quality products and more economical and environmentally friendly and healthy fabrication processes required by the basic industries. The strategy of the refractory technology to face such changes has moved towards the design of materials that resist by experiencing "in situ" microstructural modifications originated by their interaction with the environment. In this sense, modern refractories are the most performing example of smart and self-healing materials.

Regarding the thermochemical requirements, refractories are fabricated using natural raw materials and fabrication temperatures have to be economically competitive. Thus, even though it is possible to envisage refractory compositions with major phases thermodynamically compatible with the environment, it is not possible to totally prevent corrosion. Therefore, the microstructures of refractories are designed to limit the penetration depth of the corrosive agents and/or to produce protective reaction products. One of the most successful examples of such design is the development of fusion cast AZS (alumina–zirconia–silica) blocks, which, in words of Profs. Lee and Moore "was a critical advance for the glass industry, enabling glass-tank campaigns to be extended to their current length of more than a decade" [1]. The special eutectic microstructure with low porosity of AZS blocks limits the accessibility of the corrosive glass. In addition, dissolution of alumina, which is the first phase to be dissolved followed by zirconia [2], leads to the formation of a high viscosity glass boundary layer which further limits corrosion.

In order to fulfil the thermomechanical requirements, refractory products are heterogeneous materials which fracture deviates from pure linear elastic. As it has been well documented [3], the interaction of the heterogeneous microstructure with the crack leads to several energy-consuming processes ahead (process zone) and behind (process wake) the crack tip which avoid brittle failure. Crack deflection and multiple crack branching are usually observed in the frontal process zone, grain bridging and friction of crack faces occur in the process wake zone and the microcracking process zone occurring at the front accompanies crack propagation. As a result, toughness of refractories increases for increasing crack extension. Besides this rising R-curve fracture behaviour, refractory microstructures are designed to be strain tolerant to limit stress development

under imposed mechanical deformations and temperature spatial and temporal changes. In principle, phases with low Young's modulus and thermal expansion would be desirable; however, in refractory selection there are always specific compositional constraints to fulfil depending on the application. Low stiffness microstructures can be reached by selecting low Young's modulus phases as constituents and/or incorporating pores and cracks. In addition, limited crack networks can be developed in heterogeneous microstructures under subcritical conditions of temperature variations [4]. Cracks have to be controlled in order to avoid early failure and limit corrosion.

Phase equilibrium diagrams are a powerful tool for the selection of refractory compositions to fulfil thermochemical requirements while initial screening of the expected mechanical and thermal properties can be done by using simple relationships derived from the Minimum Solid Area (MSA) models and linear-elastic mechanics.

This work discusses the main role of the ZrO_2–MgO–CaO and ZrO_2–MgO–CaO–SiO_2 systems in the field refractories. In particular, the guidelines for the formulation of calcium zirconate (CZ, $CaZrO_3$)-based materials for the cement industry considering the thermochemical and thermomechanical requirements are addressed. The effect of composition on the microstructural development, the mechanical behaviour and the corrosion resistance against cement clinker is also discussed.

Refractories for cement kilns

Portland cements are fabricated in rotary kilns by reaction of natural raw materials at temperatures around 1450 °C. The major raw material is limestone ($CaCO_3$) and minor ones to be the silica (SiO_2) sources can be clay, sand, iron ore, shale, fly ashes or slags, as well as mixtures of them. The final product, called "clinker", is basically formed by four crystalline phases: alite (Ca_3SiO_5), belite (β-Ca_2SiO_4), tricalcium aluminate ($Ca_3Al_2O_6$) and ferrite ($Ca_2(Al_xFe_{2-x})_2O_5$). As minor common components are Na_2SO_4, K_2SO_4, $CaSO_4$ and KCl, the process involves aggressive basic environments and atmospheres with high alkali and sulphur contents. Consequently, the microstructure and phase composition of the refractories of the work zone of the kilns can be strongly modified.

Magnesia–chrome refractories (from silicate bonded to direct bond) present high resistance to corrosion by cement clinker because they are capable of developing in situ protective coatings by reaction with the constituents of the clinker. Therefore, they have been used in the upper transition and burning zones of rotary kilns for a long period. However, refractory wastes with more than 5 mg/l of Cr are forbidden in European and USA legislations due to the carcinogenic issues of hexavalent chromium (CrO_4^{2-}) [5].

Magnesia (MgO) aggregates and matrices of magnesia and magnesium-aluminium spinel ($MgAl_2O_4$) have been developed and used in the cement industry to substitute the chrome-based materials. In Europe alone, some 1250 million tonnes of basic shapes were manufactured in 2019, of which 14%, that is 175 million tonnes, were destined for the cement and lime industry (http://www.pre.eu/). Nevertheless, the composition of the most common commercial materials is
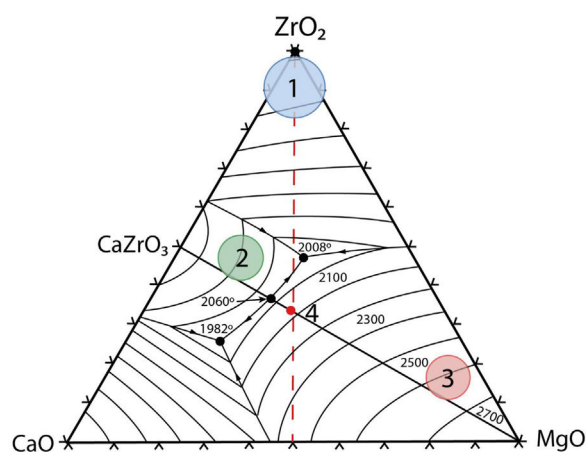

Fig. 1 – ZrO_2–MgO–CaO phase equilibrium diagram. The compositions of the main groups of refractories described in the text are indicated. Group 1 zirconia based materials; Group 2 rich calcium zirconate materials; group 3 rich magnesia materials; Point 4 dolomite-zirconia materials.

not an adequate one from the stand point of thermodynamics because even the most pure materials would form liquids at relatively low temperatures ($\approx$ 1400 °C) when combined with the components of cement, as it can be derived from the phase equilibrium relationships in the system Al_2O_3–CaO–SiO_2–MgO [6,7]. In fact, magnesia-spinel refractories present relatively low corrosion resistance under the work conditions in the cement kilns. Thus, development of new chrome-free linings for cement rotary kilns is one of the most important subjects in the refractory field from the view point of environmental protection [1].

MgO–$CaZrO_3$ based refractories have been suggested as chrome free refractories to replace not only magnesia – chromite, but also magnesia over saturated spinel refractories. MgO–$CaZrO_3$ based refractories are an attractive alternative due to the high temperatures for liquid formation in the MgO–$CaZrO_3$-rich area of the MgO–CaO-ZrO_2–SiO_2 system ($\approx$ 1550 °C) [6–8].

Thermodynamic considerations

The system ZrO_2–MgO–CaO

The ternary system zirconia-magnesia-lime is a key one in refractory technology due to the high temperatures for liquid formation involved. The *liquidus* surface of this ternary system [9] is plotted in Fig. 1. It is clear the high temperatures involved in this system, with a ternary (ZrO_2–MgO–$CaZrO_3$) eutectic at 2008 °C and a maximum temperature of 2060 °C for the real binary MgO–$CaZrO_3$ (Table 1). Ideal pure biphasic MgO–$CaZrO_3$ materials would be adequate for high temperature applications up to 2060 °C.

Well known commercial refractories with compositions within this ternary diagram are based on tetragonal + cubic zirconia (t + c ZrO_2, crucibles or nozzles for the steel industry), MgO (glass regenerators, steel and cement production) and MgO·CaO (electrical arc furnaces for steel).

Table 1 – Solid state compatibility relationships in the CaO–ZrO$_2$–MgO–SiO$_2$ system (Figs. 1 and 2) with the corresponding temperatures and types of the invariant points.

Compatible phases	Invariant point	
	Type	T (°C)
MgO-CZ	Eutectic	2060
MgO-CZ-C$_3$S-CaO	Peritectic	1740
MgO-CZ-C$_3$S-C$_2$S	Peritectic	1710
MgO-CZ-C$_3$MS$_2$-C$_2$S	Peritectic	1555
MgO-ZrO$_2$-M$_2$S-CMS	Peritectic	1485
MgO-CZ-Z-C$_3$MS$_2$	Peritectic	1475
MgO-ZrO$_2$-CMS-C$_3$MS$_2$	Eutectic	1470

CZ: CaZrO$_3$; C$_3$S: Ca$_3$SiO$_5$; C$_2$S: Ca$_2$SiO$_4$; M$_2$S: Mg$_2$SiO$_4$; C$_3$MS$_2$: Ca$_3$MgSi$_2$O$_8$; CMS: CaMgSiO$_4$.

Calcium zirconate (CaZrO$_3$, CZ) is the stable compound in the ZrO$_2$–CaO quasi-binary system. CZ has perovskite structure and bears orthorhombic crystalline lattice; it has received great attention due to its unique electrical properties associated to the perovskite structure. In the field of refractories, calcium zirconate has a high potential interest due to its high melting point ($\sim$2340 °C) and the fact that it does not present polymorphic transformations up to very high temperature (1959 °C) [10].

CZ-based materials have been proposed for crucibles and as investment casting moulds due to their thermodynamic compatibility with metals such as Ti-alloys. Advanced refractories for titanium metallurgy based on calcium zirconate with improved thermomechanical properties have been proposed and developed by Aneziris et al. [11–15].

CZ-based refractories have been also proposed as substitutes of the Cr-containing materials for the cement kilns [16]. These materials present high refractoriness and thermodynamic compatibility with the constituents of cement clinker [6,7] and lower thermal conductivity than MgO-compositions due to the low conductivity of CaZrO$_3$ [17].

Synthesis of CaZrO$_3$

Even though synthetic calcium zirconate based materials are being used for a broad range of applications since the last decades of the twentieth century, the natural analogue of CaZrO$_3$ was not reported until 2008 because of its rarity [18]. The low amounts of natural CaZrO$_3$, in spite of the relatively high amounts of Zr and Ca in natural systems, is due to its high crystallization temperature and the high activity of Si in many natural systems, which lead to the formation of zircon ZrSiO$_4$, thus decreasing Zr activity.

Due to the scarceness of natural CZ, it has to be synthesized. The most used method is the solid-state reaction of equimolar CaO and m-ZrO$_2$ mixtures, which is thermodynamically favourable at all temperatures [19]. In order to proceed reaction once CaZrO$_3$ is formed, the diffusion of Ca^{2+} ions through the newly-created CaZrO$_3$ is required [20]. In addition, the reaction involves a significant decrease of density, $\approx$ 41 and 45% for monoclinic and tetragonal

ZrO$_2$, respectively (theoretical density = 3.34, 6.30, 6.10 and 4.47 g/cm^3 for CaO, m-ZrO$_2$, t-ZrO$_2$ and CaZrO$_3$, respectively).

As a consequence of the characteristics of the solid-state reaction, relatively high temperatures and fully homogeneous mixtures of sub-micrometre raw materials are needed to avoid the presence of free lime and high porosity in the reacted materials.

The specific economic and technological features of refractory production make it impossible to fulfil the above described requirements for the fabrication of CZ by solid state reaction. Dense grains of CaZrO$_3$ refractory grades made by electric arc melting for refractory applications have been developed and used as refractory constituents [11]. The initial composition has to be controlled due to evaporation of CaO during the melting process which leads to the presence of c-ZrO$_2$ than might contaminate the liquid metal [13].

Reaction sintering [21] is an alternative sintering process in which chemical reaction between the constituents of the green compact and its densification occur during the same thermal treatment. It is an adequate technique for processing multicomponent materials. Major advantage of reaction sintering is the elimination of additional thermal and milling treatments needed to fabricate powders with the characteristics required in the final material. Therefore, it is an attractive industrial process for cost-saving widely used in the field of traditional ceramics, in which carbonates are frequent raw materials. In the same way, the use of naturally occurring minerals is an attractive alternative for the production of CaZrO$_3$–MgO-based refractories. Minerals with consistent chemical composition as dolomite (CaMg(CO$_3$)$_2$), baddeleyite (ZrO$_2$) or zircon (ZrSiO$_4$, ZS), are economically suitable reactants. This alternative approach has been used for the processing of different CZ-MgO-based materials.

Composites of CaZrO$_3$, ZrO$_2$ and MgO have been developed by the reaction sintering of baddeleyite (ZrO$_2$) and dolomite (CaMg(CO$_3$)$_2$) mixtures at temperatures above 1300 °C [22,23]. The stable polymorph of ZrO$_2$ in such compositions is the cubic one, c-ZrO$_2$, which is stabilized by CaO and MgO. The amount of CaO that enters in solid solution is significantly higher than that of MgO (e.g.: $\approx$ 20 and 5 mol% of CaO and MgO, respectively, at 1420 °C) [8]. Decomposition of dolomite at temperatures higher than 800 °C originates highly reactive nanometric particles of CaO, which readily react with ZrO$_2$ [24].

Adequate grain size and homogeneity of the raw materials are needed to avoid the presence of free lime in the final material. In addition, strict control of the thermal cycle has to be performed in order to eliminate the high porosity from carbonate decomposition in the reacted material and to accommodate the expansive formation of calcium zirconate [21,24]. When conventional constant heating rate sintering is used shrinkage variations at low temperatures are relatively large and non-monotonous. As a consequence, materials processed using conventional thermal treatment schedules are highly porous [23]. Dense calcium zirconate-magnesia composites can be reached using rate-controlled sintering [21,22].

ZrO$_2$ powders are relatively expensive synthetic raw materials. An alternative source of ZrO$_2$ is zircon (ZrSiO$_4$), which has also successfully been used to fabricate CaZrO$_3$-based
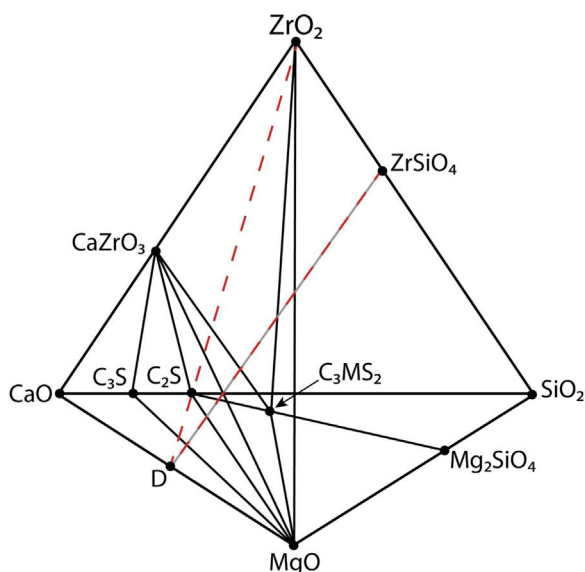
Fig. 2 – Schema of the CaO-ZrO$_2$–MgO–SiO$_2$ phase equilibrium system showing the solid state compatibility relationships in the CaO-rich region. The summary of the compatibilities and the corresponding invariant points are shown in Table 1. C$_3$S: Ca$_3$SiO$_5$; C$_2$S: Ca$_2$SiO$_4$; C$_3$MS$_2$: Ca$_3$MgSi$_2$O$_8$.

dense materials [25] and refractories [16]. The particle size of the raw materials used and in particular, the presence of agglomerates determine the quality of the final material fabricated by reaction sintering [26].

The system ZrO$_2$–MgO–CaO–SiO$_2$

The design of compositions on the basis of phase equilibrium diagrams can be done considering only the major constituents when dealing with high purity raw materials. However, additional components are required for the selection of compositions in the case of natural raw materials. In order to simplify the analysis, only the main impurities are included in a first approach. Thus, the main additional component to be considered for the analysis of CZ-MgO compositions from the above described minerals is SiO$_2$, which is the main impurity in natural dolomites and a major constituent of ZrSiO$_4$.

Fig. 2 is a schema of the CaO-ZrO$_2$–MgO–SiO$_2$ system showing the solid-state compatibility relationships in the region rich in CaO [27]. In Table 1, these compatibilities are summarized together with the corresponding invariant points.

Apart from the relatively high temperatures for liquid formation discussed above, the interest of MgO–CaZrO$_3$ based materials for the cement industry is due to the compatibility of MgO and CaZrO$_3$ with the major phases of Portland cement: alite (C$_3$S, Ca$_3$SiO$_5$) and belite (C$_2$S, Ca$_2$SiO$_4$), clearly shown in Fig. 2.

Additional facts to be considered when choosing refractory compositions on the basis of these compatibilities are the characteristics of the constituents; in this sense, it would be necessary to eliminate those with free CaO and C$_3$S due to the high hydration tendency of these compounds [16,22].

The present authors have extensively analyzed the mechanisms involved in the reaction sintering process of MgCa(CO$_3$)$_2$–ZrSiO$_4$ [25,26] and MgCa(CO$_3$)$_2$–ZrO$_2$ [22] mixtures to reach dense and fine grain materials. The information supplied by the ternary MgO–CaO–ZrO$_2$ and quaternary MgO–CaO–ZrO$_2$–SiO$_2$ systems was used for tailoring the composition and adequate characteristics of the starting powders and thermal cycles were selected to control porosity. When considering the fabrication of commercial refractories, the characteristics of the thermal cycles are limited by industrial requirements. In this case, the starting granulometry of the mixtures as a whole has to be adjusted to obtain optimum microstructures [16]. In addition, relatively high purity and reliable raw materials are required to prevent the formation of undesired minor phases and limit corrosion.

Thermomechanical considerations

In order to assure the structural integrity of refractories during use it is necessary to design microstructures that stand the extreme thermomechanical solicitations without extensive cracking. For this purpose, the initiation of cracks and, more importantly, their propagation must be controlled. In general, refractories present relatively low strength, i.e.: resistance to crack initiation, and their microstructures have to be designed for resistance to crack propagation, thus, for toughening mechanisms acting in the wake zone [4].

The main microstructural features that influence the resistance of materials to initiation of fracture are different from those that regulate crack propagation. In the case of refractories, it has been demonstrated that the characteristics of the aggregates determine toughness for crack initiation while, the presence of microstructural features capable for toughening by crack arresting and deflection are needed for high values of work of fracture [3].

In order to optimize the resistance of refractories to crack initiation, high toughness aggregates have to be envisaged. Moreover, aggregates that present higher strength than the matrix are needed for limiting crack propagation. CZ-MgO based refractories could be constituted by aggregates of CZ or of MgO due to the similarity between the toughness values of well-designed and processed CaZrO$_3$ [28] and MgO [29] materials ($\approx$2.2–2.6 MPa m$^{1/2}$).

In addition to assure the toughening capability of the aggregates, the characteristics of the boundaries between them and the matrix have to be controlled. In general, weak interfaces are sought to keep the potential of aggregates for crack deflection. Chemical compatibility between the main constituents of the aggregates and those of the matrix is needed to avoid extensive reaction between the matrix and the aggregates and the associated material continuity.

One of the main issues in ceramics is that of thermal stresses developed during temperature changes due to incompatible strains between the constituents [30]. Such strains are due to differences between thermal expansion and/or volume changes associated to phase transitions or reactions. The developed stresses might lead to cracking, and even to the complete failure of the material, as well as to the modification of the characteristics of the boundaries between the

Table 2 – Formulation and major constituents of CaZrO$_3$–MgO compositions from natural raw materials.

Compatible phases	Equation and reference	Mineralogical composition (wt.%)				
		CaZrO$_3$	MgO	C$_2$S	C$_3$MS$_2$	c-ZrO$_2$
MgO-CZ	1 [37,38]	80	20	–	–	–
MgO-CZ-calcium	2 [36](1 wt.% total impurities)	79	18	–	3	1
silicates (minor)	2 [36](6 wt.% total impurities)	55	14	–	13	18
MgO-CZ-C$_2$S	3 [25]	31	27	42	–	–
MgO-CZ-C$_3$MS$_2$	4 [25]	35	20	–	45	–
MgO-CZ-C$_3$MS$_2$-C$_2$S	5 [16]	40	21	13	26	
MgO-CZ-C$_3$MS$_2$-c-Z	6 [16]	24	16		44	16

The mineralogical composition is calculated by rational analysis using the corresponding equation. CZ: CaZrO$_3$; C$_3$S: Ca$_3$SiO$_5$; C$_2$S: Ca$_2$SiO$_4$; M$_2$S: Mg$_2$SiO$_4$; C$_3$MS$_2$: Ca$_3$MgSi$_2$O$_8$; CMS: CaMgSiO$_4$.

Table 3 – Young's modulus, E, and average thermal expansion coefficient between 298 and 1675 K, α, of the phases present in CZ-MgO based materials.

Material	E (GPa)	$\alpha_{298-1675\ K}(\times 10^{-6}\ K^{-1})$
CaZrO$_3$	228 ± 17[a]	≈10.4[c]
MgO	284 ± 9[a]	≈13.5 [16]
c-ZrO$_2$ (CaO)	256 ± 21[a]	≈10 [16]
Ca$_3$Mg(SiO$_4$)$_2$	116 [25]	≈7.4 [25]
CMSZ glass	89[b]	–

[a] E actual values determined by nanoindentation [32].
[b] E Calculated for MgO–SiO$_2$–CaO glass [32].
[c] Crystalline average [6].

material constituents. Microcracking occurs in materials with particle sizes over the critical one while stresses remain as residual stresses for finer grained materials [31]. The adequate manipulation of residual stresses is the basis of most toughening mechanisms responsible for the excellent mechanical behaviour of many ceramics in use.

The values of a Young's modulus and thermal expansion coefficients of the phases present in the CaZrO$_3$–MgO- based compositions (Table 2) are collected in Table 3 [6,16,25,32]. Data for Ca$_2$SiO$_4$ are not available due to the difficulty of fabrication of single-phase materials. This compound presents different polymorphs as a function of temperature. In particular, it experiences a martensitic transformation from β-Ca$_2$SiO$_4$ to γ-Ca$_2$SiO$_4$ with a large associated volume expansion (11%) on cooling [33] that might lead to extensive microcracking and eventually to the failure of the single-phase materials. The amounts of Ca$_2$SiO$_4$ in refractory compositions have to be limited in order to avoid extensive cracking of large particles.

As discussed above, thermal expansion mismatch between the constituents of ceramic materials and, in particular, of refractories, is a key issue for the design of composition and microstructure. During the high temperature treatments of fabrication of shaped refractories or the high temperature reactions after installation in unshaped ones, mismatch between the expansion of different phases can be accommodated by mass transport mechanisms. Contrarily, strains cannot be accommodated from temperatures at which mass transport is arrested on cooling. The thermal expansion coefficients of c-ZrO$_2$, Ca$_3$Mg(SiO$_4$)$_2$ and the crystalline average for CaZrO$_3$ are lower than that of MgO. Therefore, the expected values of the thermal expansion coefficients of the composi-

tions summarized in Table 2 will be lower than that of MgO. On the contrary, thermal expansion of the multiphase compositions will be higher or similar to that of CaZrO$_3$. For instance, calculations using the Turner's equation give values between 9.4 and 11.0 × 10^{-6} K^{-1} for the ternary compositions prepared using zircon and dolomite as raw materials [26].

Considering the expected thermal expansion values in the discussed system, shrinkage of the aggregates will be higher or lower (or similar) than that of the matrices for MgO and CaZrO$_3$ aggregates, respectively. Thus, thermal stresses will develop perpendicular (radial stresses) or parallel (tangential stresses) to the boundaries between the matrix and the MgO or CaZrO$_3$ aggregates, respectively, as schematized in Fig. 3a, b. For particle sizes over the critical one, such stresses will lead to microcracking and, if cracking does not occur, they will add to the applied external stresses during use. The expected microcrack networks are schematized in Fig. 3c, d.

From the structural integrity stand point, radial stresses leading to circumferential microcracking, such as those occurring for MgO aggregates (Fig. 3a, c), are preferred as compared to tangential stresses at the boundary of the CaZrO$_3$ ones that would originate radial microcracks (Fig. 3b, d) traversing the matrix, thus, being more prone to originate material failure.

From the existing toughening mechanisms, microcracking and grain bridging and friction of crack faces are sought in refractories in order to improve their resistance to thermal and mechanical cycles. As discussed above, the residual stress field for MgO aggregates is adequate for the development of a controlled microcrack network, thus, microcracking toughening would be expected. The most efficient toughening mechanisms are grain bridging and friction of crack faces for which the toughening level is determined by the fracture stress, the elastic modulus and the size of the ligaments. The stiffer MgO aggregates would be preferred as compared to CaZrO$_3$ because they would present higher resistance to the opening of the crack. Moreover, bridging and friction are conditioned by the state of residual tensions of the ligament and the matrix and the presence and geometry of microcracks, since these determine whether the crack surrounds or draws nearer to the toughening ligament. In this sense, MgO aggregates are also more suitable than CaZrO$_3$ ones due to the characteristics of the residual stresses described (Fig. 3).

The approximation of low thermal expansion particles surrounded by a high thermal expansion matrix, was proposed
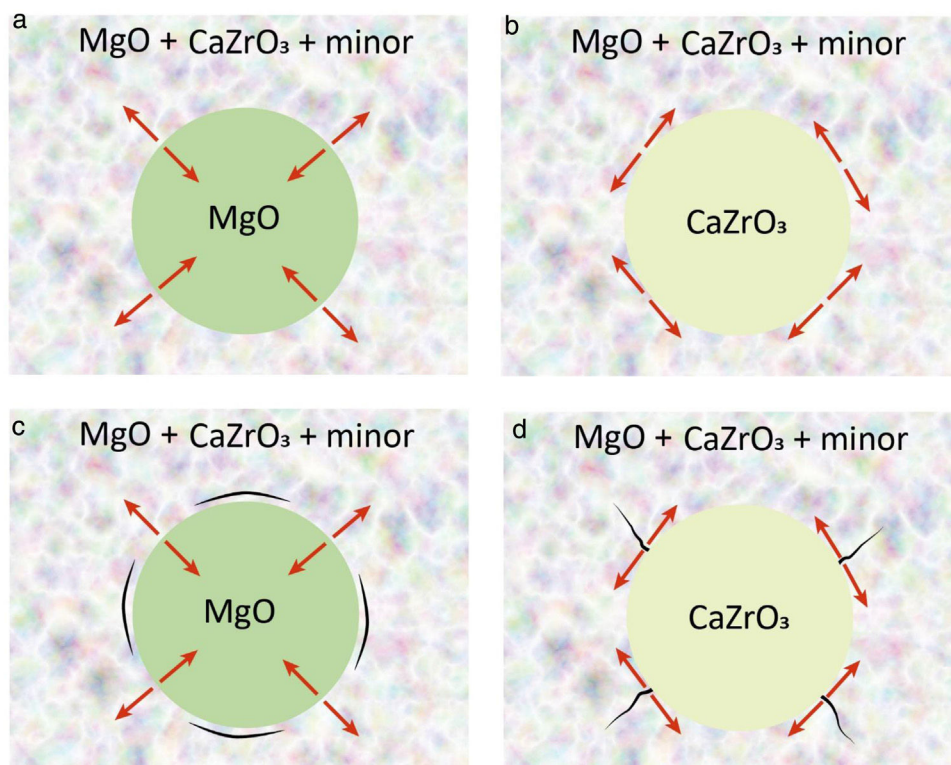
Fig. 3 – Schema of the potential designs of MgO–CaZrO₃ refractories from natural raw materials. (a) MgO aggregates with radial stresses (red arrows) developed at the grain boundaries. (b) CaZrO₃ aggregates with tangential stresses (red arrows) developed at the grain boundaries. (c) Circumferential microcrack network black expected for MgO aggregates. (d) Tangential microcrack network black expected for CaZrO₃ aggregates.

by Axel et al. [34] to improve the thermal shock resistance of MgO. These researchers developed model composites constituted by MgO matrices with Mg-Al spinel particles dispersed. Such materials developed networks of cracks perpendicular to the spinel particles which drastically decreased the matrix strength even in the case of very fine particles [29]. Moreover, magnesia-spinel materials present low resistance to corrosion in cement kilns because their compositions are not adequate from the stand point of thermodynamics. A detailed observation of the Al_2O_3–CaO–SiO_2–MgO phase equilibrium relationships [6–8] shows that MgO-spinel compositions would develop liquids at very low temperatures (<1350 °C) when combined with the components of cement.

CZ-MgO-based refractories

As discussed above, MgO aggregates are preferred when dealing with CZ-MgO refractories due to thermomechanical issues. Moreover, MgO aggregates of a wide range of qualities are commercially available. As the fine grains that constitute the matrix of a refractory are much more reactive than the aggregates, a general rule for refractory design is that the matrix composition has to be more resistant to corrosion than that of the aggregates. A general statement on the high resistance to corrosion by Portland cement of CaZrO₃–MgO based matri-
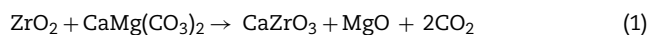
ces can be done because both phases are compatible with the major phases of cement clinker (Ca_3SiO_5 and Ca_2SiO_4).
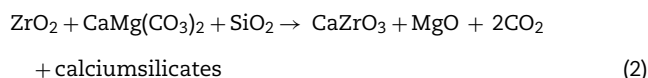
Matrix

Different approaches have been undertaken in our group, in the last years, to formulate CZ-MgO matrices, as summarized in Table 2. In principle, matrices with compositions from Table 2, excluding those containing Ca_2SiO_2, would be adequate for the lining of cement kilns. Regarding the major constituents in the matrix composition, different formulation scenarios have been considered:

a) Baddeleyite – dolomite mixtures

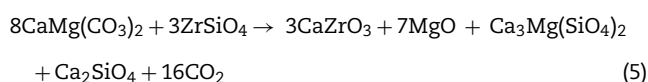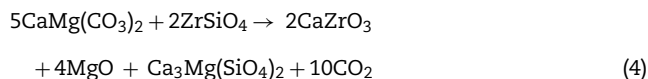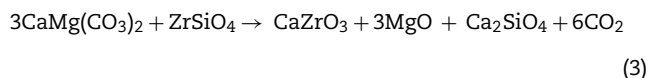High purity baddeleyite – high purity dolomite mixtures (Eq. (1)):

$$ZrO_2 + CaMg(CO_3)_2 \rightarrow CaZrO_3 + MgO + 2CO_2 \qquad (1)$$

High purity baddeleyite ZrO_2 – medium purity (>94 wt.%) dolomite (SiO_2 as main impurity) mixtures (Eq. (2)):

$$ZrO_2 + CaMg(CO_3)_2 + SiO_2 \rightarrow CaZrO_3 + MgO + 2CO_2$$
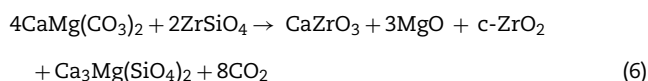$$+ calciumsilicates \qquad (2)$$

As observed in Table 2, the major phases and their relative amount in the materials is dramatically changed for increasing amounts of impurities.

b) Zircon – dolomite mixtures

High purity $ZrSiO_4$ and dolomite mixtures (Eqs. (3–6)):

$$3CaMg(CO_3)_2 + ZrSiO_4 \rightarrow CaZrO_3 + 3MgO + Ca_2SiO_4 + 6CO_2 \tag{3}$$

$$5CaMg(CO_3)_2 + 2ZrSiO_4 \rightarrow 2CaZrO_3$$
$$+ 4MgO + Ca_3Mg(SiO_4)_2 + 10CO_2 \tag{4}$$

$$8CaMg(CO_3)_2 + 3ZrSiO_4 \rightarrow 3CaZrO_3 + 7MgO + Ca_3Mg(SiO_4)_2$$
$$+ Ca_2SiO_4 + 16CO_2 \tag{5}$$

For dolomite/zircon ratios lower than 5/2, c-ZrO_2 appears as additional phase, e.g.: Eq. (6):

$$4CaMg(CO_3)_2 + 2ZrSiO_4 \rightarrow CaZrO_3 + 3MgO + c\text{-}ZrO_2$$
$$+ Ca_3Mg(SiO_4)_2 + 8CO_2 \tag{6}$$

Even in the case of high purity raw materials, additional calcium silicate phases are formed in all matrices formulated with zircon and dolomite. The additional phases are merwinite (C_3MS_2, $Ca_3Mg(SiO_4)_2$) and/or belite (C_2S, Ca_2SiO_4). In addition to granulometry and impurities, the ratio dolomite/zircon is a main design parameter for these materials in which the total amounts of the desired phases, Ca_2SiO_4 and MgO, sharply decrease as compared to materials formulated with ZrO_2. Examples of phase compositions of matrices in which $CaZrO_3$ and MgO are present and have different ratios of dolomite/zircon are collected in Table 2.

Fig. 4 shows characteristic microstructures of materials designed on the basis of Eq. (2) from dolomites of high (Fig. 4a) and low (Fig. 4b) purity [22]; both materials have $CaZrO_3$ and MgO as major phases. When the high purity dolomite was used, very low amounts (<4 wt.%) of c-ZrO_2 and merwinite ($Ca_3Mg(SiO_4)_2$) were present were in the material as secondary phases. For the low purity dolomite, c-ZrO_2, merwinite ($Ca_3Mg(SiO_4)_2$), monticellite($CaMgSiO_4$) and dicalcium silicate (Ca_2SiO_4) were present as minor phases. In addition, significant amounts of residual glass were found in this latter material, in which significant grain growth due to liquid formation at high temperature occurred, especially when it was treated at 1450 °C.

Corrosion

In principle, the compatibility between the compositions of the proposed CZ-MgO-based matrices and the main phases of the clinker would assure their high corrosion resistance. However, as it will be discussed below, the corrosion processes
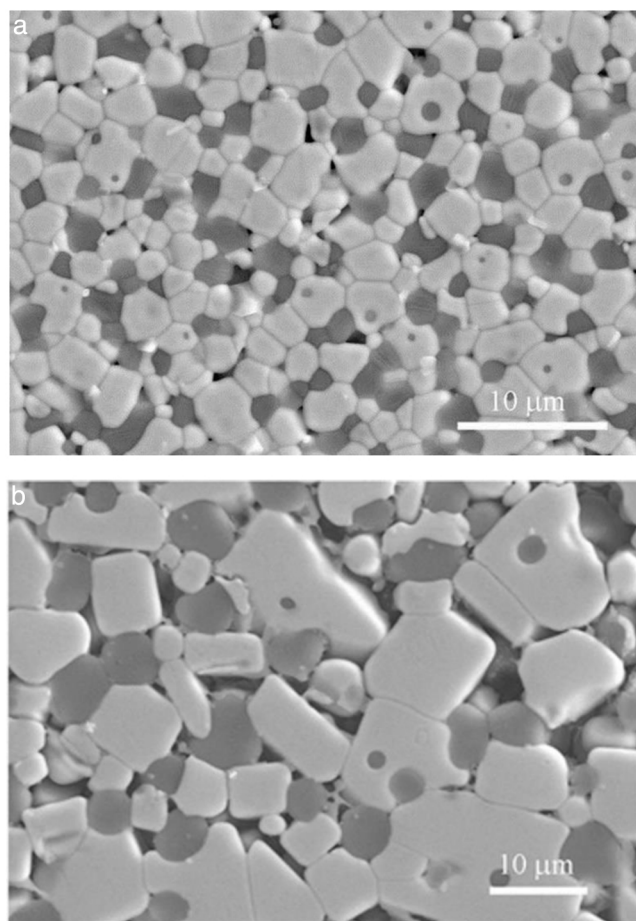

Fig. 4 – Characteristic microstructures of CaZrO₃–MgO materials designed according to Eq. (2) from dolomites of different purities sintered at 1450 °C – 2 h [22]. The darkest grains are MgO and the major grey phase is CaZrO₃. FE-SEM micrographs of polished and thermally etched surfaces. (a) High purity dolomite. (b) Low purity dolomite.

in real systems are determined by the dissolution of the refractory constituents in the calcium silicate rich liquid phases of the clinker.

The corrosion of MgO–CaZrO₃-based matrices by Portland cement at 1450 °C and 1500 °C has been established by the reaction method [35–38]. In this method, the diffusion couples are made by placing small cylinders (1.5 mm diameter × 4 mm thickness) of the corrosive agent, shaped by pressing manually the power in the dye, on polished surfaces of the test material. Then, the diffusion couples are heated in a hot stage microscope for dynamic tests or in an electrical furnace for long term tests at the considered temperature. After the tests, the specimens are mounted in an epoxy resin, cut transversally, polished and analyzed using reflected light optical microscopy (RLOM), and field emission scanning electron microscopy with energy dispersive X-ray analysis (FE-SEM/EDS).

Fig. 5 a shows a characteristic image of diffusion couples clinker–CaZrO₃–MgO based matrices after testing. For well-designed matrices, the clinker cylinder shrinks keeping its original shape and maintaining the initial contact angle ($\approx 90°$) with the substrate until the end of the experiment, revealing
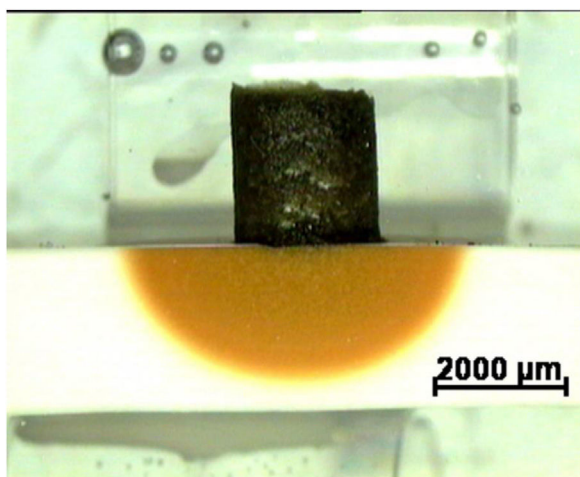
Fig. 5 – Characteristic image of a cross section of a reaction couple used to study corrosion showing the experimental arrangement: clinker (dark) and matrix specimen (clear). The yellowish semicircular area reflects the penetration of Fe from the clinker. The couple is embedded in a resin before polishing (light green). Reflected light optical microscopy.

Fig. 6 – Corrosion of CaZrO₃–MgO matrices fabricated from zirconia and dolomite (Table 2, Eq. (2)). Micrographs of the polished cross sections of diffusion couples cement clinker-matrix after a static test at 1450 °C during 2 h. The interfaces between the clinker (upper part) and the matrix (lower part) are observed. Light grey: CaZrO₃; dark grey: MgO. FE-SEM back scattered images. (a) Material fabricated using a high purity dolomite. (b) Material fabricated using a low purity dolomite. Large MgO grains are observed at the interface.

limited reaction. The coloured area in the substrate underneath the clinker corresponds to diffusion of Fe. As Fe is the clinker specie that diffuses the farthest into the substrate, as revealed by EDS, this coloured zone can be identified as the reaction one.

Typical clinker compositions (e.g.: 5.7 wt.% Al_2O_3; 3.9 wt.% Fe_2O_3; 66.06 wt.% CaO; 21.25 wt.% SiO_2, 1.5 wt.% MgO) include small amounts of Al_2O_3 and Fe_2O_3 in addition to the main clinker constituents (CaO and SiO_2). Therefore, in spite of the invariant points of the subsystem $MgO–CaZrO_3–Ca_3SiO_5–Ca_2SiO_4$ reaching temperatures of 1700 and 1750 °C (Table 1), the temperature of first liquid formation in the clinker is decreased down to ≈1200 °C [39], so that corrosion is dominated by the clinker and refractory impurities.

The attack of the clinker occurs through the diffusion of the calcium silicate rich liquid phases (Ca, Si, Fe, Mg) of the clinker through the pores, liquids and grain boundaries of the refractory. Reaction of the clinker phases with the major constituents of the refractory ($CaZrO_3$, MgO) leads to the dissolution of these later even in model high purity materials [37,38].

The corrosion resistance of real refractory matrices, which containing silica and minor impurities, is discussed in which follows. In this regard it is important to highlight the small compositional region of the primary field of $CaZrO_3$ as compared to that of MgO in the quaternary system $CaO–MgO–ZrO_2–SiO_2$ [22,35]. This feature makes the refractory composition to move readily from the $CaZrO_3$ primary field to that of MgO due to minor impurities in the raw materials and/or the corrosion process.

Fig. 6 shows interfaces of diffusion couples clinker/matrix for matrices designed following Eq. (2) with dolomites of high (Fig. 6a) and low (Fig. 6b) purities [22,36]. MgO grains larger than those in the original microstructures are observed at the inter-
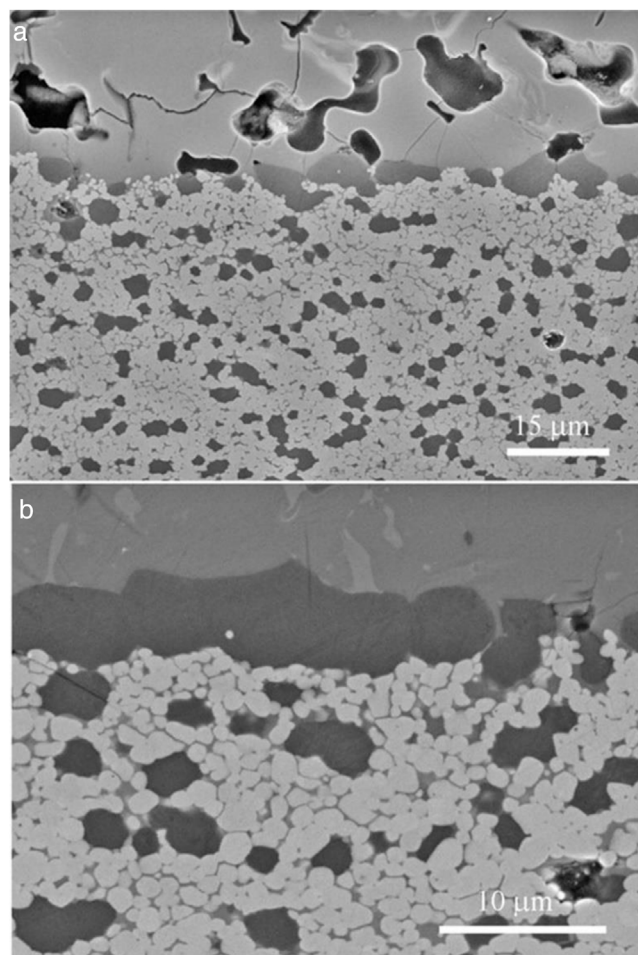
faces in both cases. The results of the EDS-SEM microanalysis demonstrated that these large grains have Fe in solid solution, being their composition variable, $Mg_{1-x}Fe_xO$. In the material with higher amount of impurities these grains formed a layer (Fig. 6b) and the penetration depth of the clinker in this material was lower than in the high purity one.

The observed microstructures suggest that in the initial stages of corrosion the liquid phase in the clinker penetrates the material dissolving CZ and MgO. For larger times, the composition at the interface moves to the equilibrium one in which MgO and liquid are the expected phases because the refractory compositions lie in the primary field of MgO. Iron from the clinker enters in solid solution in the MgO grains precipitated from the liquid that grow due to enhanced diffusion in liquid phase. At this stage the layers of $Mg_{1-x}Fe_xO$ grains act as barri-

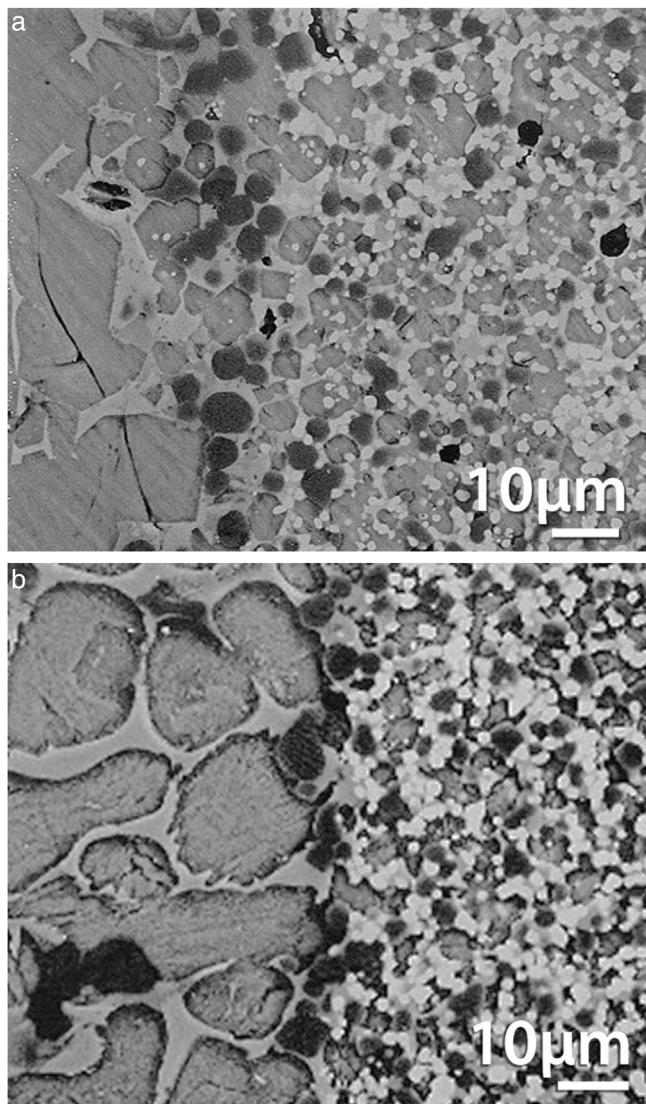**Fig. 7 – Corrosion of a CaZrO₃–MgO matrices fabricated from zircon and dolomite (Table 2). Micrographs of the polished cross section of the diffusion couple cement clinker (left)-matrix (right) after a static test at 1500 °C during 1 min. MgO (dark) and silica glass (light grey) are observed at the interface. Some small particles (CaZrO₃ or ZrO₂) are observed deeper in the matrix. FE-SEM back scattered images. (a) Material formulated according to Eq. (3). (b) Material formulated according to Eq. (4).**

between the refractory and the clinker, high amounts of glass were formed and initial corrosion of these materials was relatively high. As occurred for the purer materials, large re-precipitate $Mg_{1-x}Fe_xO$ particles were formed at the very interface refractory-reaction zone which in this case were surrounded by glass. After this interface, a reaction zone with numerous round shaped MgO (dark) and CaZrO₃ (clear) particles surrounded by liquid phases is observed in both microstructures. These particles correspond to the original constituents of the material which are partially dissolved in the multicomponent (SiO_2, CaO, Al_2O_3, Fe_2O_3, ZrO_2, MgO, etc.) liquid formed by reaction of the clinker and the material liquid phases. The efficiency of the $Mg_{1-x}Fe_xO$ particles at the interface as barriers for clinker diffusion in these materials is lower than in the purer ones due to the interaction of the liquid formed in the material with that of the clinker. However, the resistance to corrosion of these materials with relatively high silica contents was still higher than that of Mg-Al spinel tested in the same conditions [35]. This fact is explained by the higher viscosity of the liquids formed in the ZrO_2–CaO–SiO_2–MgO system, as compared to those of the Al_2O_3–CaO–SiO_2–MgO one, due to the presence of Zr from dissolution of CZ.

Refractory design

In a previous work [16], we demonstrated the feasibility of extending the reaction sintering approach to obtain MgO–CaZrO₃-based refractories from dolomite ($MgCa(CO_3)_2$) and zircon ($ZrSiO_4$) natural raw materials. The focus was to determine the main processing parameters that have to be controlled to reach defect free materials with periclase aggregates and matrices in the range of compositions of Table 2. For non-reacting systems, optimum packing in the green compacts leads to sintered materials with minimum and homogeneously distributed porosity. In the considered compositions, matrices experience extreme volume changes from relatively low temperatures (~600–800 °C) due to decarbonation of $MgCa(CO_3)_2$, and have as final compositions the result of the high temperature reactions between the initial constituents. Due to such matrix specific characteristics, the optimum microstructures, i.e. minimum porosity and adequate matrix content to constitute the bonding between the aggregates, were found for initial matrix fractions higher than those for non-reactive systems. It was also concluded that the fabrication temperatures have to be chosen considering the specific compositions of the matrices in order to avoid extensive reaction between the aggregates and the matrix components due to liquid formation.

The optimum MgO-CZ refractories developed in the previous work were constituted by MgO aggregates totally surrounded by matrices. The best mechanical behaviour occurred for matrices of composition CaZrO₃–MgO-cubic–ZrO_2–$Ca_3Mg(SiO_4)_2$ or CaZrO₃–MgO–Ca_3Mg $(SiO_4)_2$–Ca_2SiO_4. All materials had cracks around the MgO aggregates, which were developed during cooling from the sintering temperature due to differences between the thermal expansion of the aggregates and the matrices (calculated thermal expansion coefficients $\approx 10 \times 10^{-6}\,K^{-1}$). Materials with such microstructures presented stable crack growth with high

ers for further clinker penetration in the matrices preventing corrosion. In the case of relatively low silica content of the matrices, the described mechanism makes the higher impurity content to be not detrimental for the corrosion resistance [36].

The corrosion process of matrices containing higher amounts of silica is more severe due to the interaction of the liquids formed in the matrices, which also move towards the reaction interface, with those of the clinker [35]. Fig. 7 shows characteristic microstructures of the reaction zones for materials fabricated from zircon – dolomite, which contained different silicate phases (Eqs. (3) and (4)). At the interface
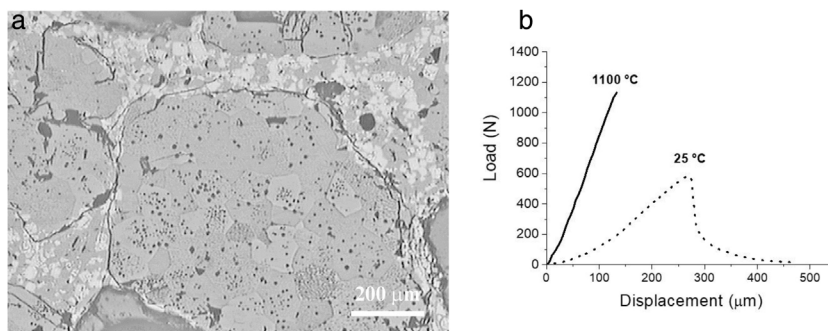
Fig. 8 – Optimised MgO-CZ refractory. (a) Characteristic microstructural features: circumferential crack surrounding a MgO aggregate. CZ (white) is observed in the matrix. Reflected light optical microscopy of a polished surface. (b) Characteristic load-displacement curves at the indicated temperatures. Specimens with modulus of rupture of 7 MPa (25 °C) and 14 MPa (1100 °C).

work of fracture (40–70 J/m^2) and medium strength values (4–6 MPa) at room temperature and linear fracture behaviour and high strength (9–15 MPa) at 1100 °C. This behaviour was attributed to microcrack opening at room temperature and closure at 1100 °C.

Fig. 8a shows an example of an optimized refractory microstructure with CZ, MgO, c-ZrO$_2$ and C$_3$MS$_2$ as final phases in the matrix (Eq. (6), Table 2) and characteristic load displacement curves recorded during bending tests are shown in Fig. 8b.

Room temperature modulus of rupture was determined by three-point bending (span 150 mm) following the procedure of EN993-6 standard, using a universal testing machine (Microtest, Spain) with stainless steel supports; reported values are the average of seven determinations and errors are the standard deviations.

Bending tests at 1100 °C (heating rate = 5 °C/min, holding time before testing 20–60 min) were performed in a specially developed mechanical testing device with high purity dense alumina supports [40] using the same loading conditions as for the room temperature tests (EN993-7). Reported values are the average of three determinations and errors are the standard deviations. All bending tests were performed in displacement control and the load–displacement curves were recorded. For room temperature tests, stable fracture was reached (Fig. 8b) and the work of fracture was calculated as the area under the curves divided by twice the cross section of the specimens.

This material presented room temperature Young's modulus ($E = 78 \pm 4$ GPa) and strength (MOR = 7 ± 1 MPa) similar to those of MgO commercial refractories ($E = 40$–106 GPa) [4] and work of fracture (WOF = 72 ± 5 J/m^2) similar to those of well-designed alumina bricks (40–140 J/m^2) [4]. Crack closure at high temperature led to high strength values (MOR = 15 ± 3 MPa).

Final remarks

The increasing severity of the working conditions of refractories together with the necessity of available and economically feasible raw materials have changed the design approaches towards materials experiencing "in situ" modifications during use. Naturally occurring minerals such as dolomite, badde-

leyite or zircon appear as attractive for the fabrication of relatively low-cost calcium zirconate-based matrices for magnesia refractories. The initial formulation of the matrices can be done using the quaternary phase equilibrium system ZrO$_2$–MgO–CaO–SiO$_2$ to reach materials with major phases compatible with the main constituents of the clinker. Lime, alite and belite should be avoided in the final materials. The clinker liquid phase together with silica and impurities in the material determine corrosion. Compositions formulated in the primary field of MgO and leading to the presence of Zr in the liquid are corrosion resistant after the initial stages. Tailoring of the thermal expansion of the matrix allows the optimization of the mechanical behaviour.

In memoriam of our friend and colleague Prof. Victor Orera.

REFERENCES

[1] W.E. Lee, R.E. Moore, Evolution of in situ refractories in the 20th century, J. Am. Ceram. Soc. 81 (6) (1998) 1385–1400, http://dx.doi.org/10.1111/j.1151-2916.1998.tb02497.x.

[2] P. Pena, E. Criado, J.J. Bakali, C. Baudín, Dynamic corrosion of Al$_2$O$_3$–ZrO$_2$–SiO$_2$ and Cr$_2$O$_3$-containing refractories by molten frits. Part II: Microstructural study, J. Eur. Ceram. Soc. 31 (5) (2011) 705–714, http://dx.doi.org/10.1016/j.jeurceramsoc.2010.11.024.

[3] A. García-Prieto, M. Dos Ramos-Lotito, D. Gutiérrez-Campos, P. Pena, C. Baudín, Influence of microstructural

characteristics on fracture toughness of refractory materials, J. Eur. Ceram. Soc. 35 (6) (2015) 1955–1970, http://dx.doi.org/10.1016/j.jeurceramsoc.2014.12.020.

[4] C. Baudín, Thermal shock behavior of ceramics: fundamentals and thermal shock resistance parameters, in: M. Pomeroy (Ed.), Encyclopedia of Materials: Technical Ceramics and Glasses, vol. 1, Elsevier, Oxford, 2021, pp. 867–878, http://dx.doi.org/10.1016/B978-0-12-803581-8.12117-4.

[5] D.J. Bray, Toxicity of chromium compounds formed in refractories, Am. Ceram. Soc. Bull. 64 (7) (1985) 1012–1016.

[6] J. White, Recent applications of phase diagrams to problems in the field of refractory materials, in: A. Alper (Ed.), Phase Diagrams, vol. IV, Academic Press, New York, 1976, pp. 233–297.

[7] P. Pena, B. Vázquez, A. Caballero, S. De Aza, Diagramas de equilibrio de fases cuaternarios. Métodos de representación e interpretación, Bol. Soc. Esp. Ceram. 44 (2) (2005) 113–122, http://boletines.secv.es/es/index.php?id=12&vol=44.

[8] A. Sircar, N.H. Brett, J. White, Phase studies in the system CaO–MgO-ZrO2–SiO2. Part II: Compatibility relations of zirconia, J. Trans. Br. Ceram. Soc. 77 (3) (1978) 77–88.

[9] S. Serena, M.A. Sainz, S. de Aza, A. Caballero, Thermodynamic assessment of the system ZrO_2–CaO–MgO using new experimental results. Calculation of the isoplethal section MgO–CaO–ZrO_2, J. Eur. Ceram. Soc. 25 (5) (2005) 681–693, http://dx.doi.org/10.1016/j.jeurceramsoc.2004.02.011.

[10] Y. Du, Z. Jin, P. Huang, Thermodynamic calculation of the zirconia-calcia system, J. Am. Ceram. Soc. 75 (11) (1992) 3040–3048, http://dx.doi.org/10.1111/j.1151-2916.1992.tb04384.x.

[11] S. Schafföner, C.G. Aneziris, H. Berek, J. Hubálková, A. Priese, Fused calcium zirconate for refractory applications, J. Eur. Ceram. Soc. 33 (15–16) (2013) 3411–3418, http://dx.doi.org/10.1016/j.jeurceramsoc.2013.07.008.

[12] S. Schafföner, C.G. Aneziris, H. Berek, B. Rotmann, B. Friedrich, Investigating the corrosion resistance of calcium zirconate in contact with titanium alloy melts, J. Eur. Ceram. Soc. 35 (1) (2015) 259–266, http://dx.doi.org/10.1016/j.jeurceramsoc.

[13] S. Schafföner, J. Fruhstorfer, C. Faßauer, L. Freitag, C. Jahn, C.G. Aneziris, Influence of in situ phase formation on properties of calcium zirconate refractories, J. Eur. Ceram. Soc. 37 (1) (2017) 305–313, http://dx.doi.org/10.1016/j.jeurceramsoc.2016.08.017.

[14] T. Qin, J. Fruhstorfer, C. Jahn, G. Schmidt, S. Schafföner, H. Jansen, C.G. Aneziris, Refractory castables for titanium metallurgy based on calcium zirconate, Mater. Des. 148 (2018) 78–86, ISSN: 0264-1275, 0261-3069, 1873-4197.

[15] S. Schaffoner, M. Bach, C. Jahn, L. Freitag, C.G. Aneziris, Advanced refractories for titanium metallurgy based on calcium zirconate with improved thermomechanical properties, J. Eur. Ceram. Soc. 39 (14) (2019) 4394–4403.

[16] A. Obregón, J.L. Rodríguez-Galicia, J. López-Cuevas, P. Pena, C. Baudín, MgO–CaZrO3-based refractories for cement kilns, J. Eur. Ceram. Soc. 31 (12) (2011) 61–74.

[17] P.M.C. Carneiro, A. Maceiras, J. Nunes-Pereira, P.D. Silva, A.P. Silva, C. Baudín, Numerical modelling of the thermal conductivity of CaZrO3–MgO ceramic composites, J. Eur. Ceram. Soc. (submitted for publication).

[18] E.V. Galuskin, V.M. Gazee, T. Armbruster, A.E. Zadov, I.O. Galuskina, N.N. Pertsev, P. Dzierżanowski, M. Kadiyski, A.G. Gurbanov, R. Wrzalik, A. Winiarski, Lakargiite CaZrO3: a new mineral of the perovskite group from the North Caucasus, Kabardino-Balkaria Russia, Am. Mineral. 93 (2008) 1903–1910.

[19] G. Oprea, Solid state reaction kinetics for the calcium zirconate synthesis, Sintering'91 Solid State Phenom. 25–26 (1992) 125–132, http://dx.doi.org/10.4028/www.scientific.net/SSP.25-26.125.

[20] S. Serena, A. Caballero, M.A. Sainz, P. Convert, J. Campo, X. Turrillas, Neutron thermodiffractometry study of calcium zirconate/magnesium oxide formation in the ZrO_2–CaO–MgO system, J. Am. Ceram. Soc. 87 (9) (2004) 1706–1713, http://dx.doi.org/10.1111/j.1551-2916.2004.01706.x.

[21] C. Baudín. Reaction Sintering, in: M. Pomeroy (Ed). Encyclopedia of Materials: Technical Ceramics and Glasses, vol., Elsevier, Oxford, 2021, pp. 278–285, https://doi.org/10.1016/B978-0-12-803581-8.11766-7.

[22] F. Booth, L. Garrido, E. Aglietti, A. Silva, P. Pena, C. Baudín, CaZrO3–MgO structural ceramics obtained by reaction sintering of dolomite-zirconia mixtures, J. Eur. Ceram. Soc. 36 (2016) 2611–2626, http://dx.doi.org/10.1016/j.jeurceramsoc.2016.03.027.

[23] J. Szczerba, Z. Pedzich, The effect of natural dolomite admixtures on calcium zirconate–periclase materials microstructure evolution, Ceram. Int. 36 (2010) 535–547, http://dx.doi.org/10.1016/j.ceramint.2009.09.025.

[24] Y. Suzuki, P.E.D. Morgan, T. Sekino, K. Niihara, Manufacturing nano-diphasic materials from natural dolomite: in situ observation of nanophase formation behaviour, J. Am. Ceram. Soc. 80 (11) (1997) 2949–2953, http://dx.doi.org/10.1111/j.1151-2916.1997.tb03218.x.

[25] J.L. Rodríguez-Galicia, C. Baudín, P. Pena, Relationships between phase constitution and mechanical behaviour in MgO–CaZrO3-calcium silicate materials, J. Eur. Ceram. Soc. 24 (4) (2004) 669–679, http://dx.doi.org/10.1016/S0955-2219(03)00268-1.

[26] J.L. Rodríguez, S. De Aza, P. Pena, Agglomerate and particle size effects on reaction sintering of zircon dolomite mixtures, Br. Ceram. Trans. 100 (4) (2001) 181–191, http://dx.doi.org/10.1179/096797801681431.

[27] S. de Aza, C. Richmond, J. White, Compatibility relationships of periclase in the system CaO–MgO–ZrO_2–SiO2, Trans. J. Br. Ceram. Soc. 73 (1974) 109–116.

[28] M. Dudek, E. Drozdz-Ciesla, Some observations on synthesis and electrolytic properties of nonstoichiometric calcium zirconate, J. Alloys Compd. 475 (1–2) (2009) 846–854, http://dx.doi.org/10.1016/j.jallcom.2008.08.020.

[29] C. Aksel, B. Rand, F.L. Riley, P.D. Warren, Mechanical properties of magnesia-spinel composites, J. Eur. Ceram. Soc. 22 (5) (2002) 745–754, http://dx.doi.org/10.1016/S0955-2219(01)00373-9.

[30] S. Bueno, C. Baudín, Mechanical behaviour of structural ceramics, Bol. Soc. Esp. Ceram. V 46 (3) (2007) 103–118, http://boletines.secv.es/upload/20070528162020.46[3]103-118.pdf.

[31] S. Bueno, C. Baudín, Aluminum titanate, structure and properties, in: M. Pomeroy (Ed.), Encyclopedia of Materials: Technical Ceramics and Glasses, vol. 2, Elsevier, Oxford, 2021, pp. 76–92.

[32] A.P. Silva, F. Booth, L. Garrido, E. Aglietti, P. Pena, C. Baudín, Young's modulus and hardness of multiphase CaZrO3–MgO ceramics by micro and nanoindentation, J. Eur. Ceram. Soc. 38 (4) (2018) 2194–2201.

[33] I. Nettleship, K.G. Slavick, Y.J. Kim, W.M. Kriven, Phase transformations in dicalcium silicate: I. Fabrication and phase stability of fine-grained β phase, J. Am. Ceram. Soc. 75 (9) (1992) 2400–2406, http://dx.doi.org/10.1111/j.1151-2916.1992.tb05592.x.

[34] C. Aksel, P.D. Warren, F.L. Riley, Magnesia-spinel microcomposites, J. Eur. Ceram. Soc. 24 (10) (2004) 3119–3128, http://dx.doi.org/10.1016/j.jeurceramsoc.2003.10.036.

[35] J.L. Rodríguez-Galicia, A.H. de Aza, J.C. Rendón-Angeles, P. Pena, The mechanism of corrosion of MgO CaZrO3–calcium

silicate materials by cement clinker, J. Eur. Ceram. Soc. 27 (1) (2007) 79–89, http://dx.doi.org/10.1016/j.jeurceramsoc.2006.01.014.

[36] F. Booth, L. Garrido, E. Aglietti, A. Silva, P. Pena, C. Baudín. Estudio del ataque por corrosión en materiales cerámicos del sistema MgO–CaZrO$_3$. Proceedings ALAFAR 2016, Manuscript 26.

[37] S. Serena, M.A. Sainz, A. Caballero, Corrosion behavior of MgO/CaZrO$_3$ refractory matrix by clinker, J. Eur. Ceram. Soc. 24 (8) (2004) 2399–2406, http://dx.doi.org/10.1016/j.jeurceramsoc.2003.07.007.

[38] S. Serena, M.A. Sainz, A. Caballero, The system clinker–MgO–CaZrO$_3$ and its application to the corrosion behavior of CaZrO$_3$/MgO refractory matrix by clinker, J. Eur. Ceram. Soc. 29 (11) (2009) 2199–2209, http://dx.doi.org/10.1016/j.jeurceramsoc.2009.01.015.

[39] E. Jak, S. Degterov, P.C. Hayes, A.D. Pelton, Thermodynamic modeling of the system Al$_2$O$_3$–SiO$_2$–CaO–FeO–Fe$_2$O$_3$ to predict the flux requirements for coal ash slags, Fuel 77 (1–2) (1998) 74–84, http://dx.doi.org/10.1016/S0016-2361(97)00137-3.

[40] C. Alvarez, E. Criado, C. Baudín, G. Duphia, H. Kelichaus, Hot modulus of rupture automatic testing machine, in: Proceedings of the UNITECR '93 Congress, Sao Paulo, Brazil: Asociación Latinoamericana de Fabricantes de Refractarios, 1993, pp. 435–441.